ENCIT 2018

ABCM Associação Brasileira de Engenharia e Ciências Mecânicas

17th Brazilian Congress of Thermal Sciences and Engineering
November 25th-28th, 2018, Águas de Lindóia, SP, Brazil

ENCIT-2018-0646
SIMULATION OF A PLANAR HEATED JET USING A WEIGHTED ESSENTIALLY NON-OSCILLATORY SCHEME

Eduardo Henrique Salermo de Lima
Rogério Gonçalves dos Santos
University of Campinas, Faculty of Mechanical Engineering
200 Mendeleyev Street, Barão Geraldo District, Campinas, SP, Brazil
dusamil@fem.unicamp.br
roger7@fem.unicamp.br

Sávio Souza Venâncio Vianna
University of Campinas, Faculty of Chemical Engineering
500 Albert Einstein Avenue, Barão Geraldo District, Campinas, SP, Brazil
savio@feq.unicamp.br

Abstract. *The present work investigates the planar heated jet using high-ordered and Essentially Non-Oscillatory scheme on the framework of direct numerical simulation of a two dimensional domain with uniform velocity profile. Numerical findings are in agreement with the current understanding of turbulent jet flows.*

Keywords: *Weighted Essentially Non-Oscillatory Scheme, Direct numerical simulation, Planar Jet*

1. INTRODUCTION

Compressible flows dominated by convection, typically found in aeronautics and combustion problems, may present discontinuous regions. Standard high-order interpolations uses a stencil with many points at once to create a polynomial function that interpolates the values in these points. If this stencil is in a smooth region the approximation will be very accurate. However, if a discontinuity is present between those points that makes up the stencil, this polynomial function will exhibit oscillations known as Gibbs phenomenon (Hewitt and Hewitt, 1979).

There are some methods like artificial viscosity (Neumann and Richtmyer, 1950), the Godunov scheme (Godunov, 1959) or the Roe scheme (Roe, 1981) to deal with discontinuities. These methods are suitable for treating Gibbs phenomenon. However, they contain large numerical dissipation in the smooth region of the solution, thus it is not recommended for numerical simulations involving turbulence (Shu, 2012). Other schemes with second order accuracy like MUSCL and Total Variation Diminishing (TVD) schemes are used to resolve compressible flow problems with discontinuities and turbulence. However, there is a compromise between the order of the method and the mesh size to numerically solve the governing equations. Thus, it is recommended to use methods with accuracy higher than second-order when solving a direct numerical simulations to reduce higher computational costs.

Harten *et al.* (1987) developed a method that is at the same time high-order accurate and non-oscillatory. Unlike standard finite difference scheme, the so-called ENO (Essentially Non-oscillatory) scheme uses an adaptive-stencil approach. Divided differences are used to assess the smoothness of the sub-stencil for the polynomial reconstruction. Liu *et al.* (1994) put forward a variation of ENO called Weighted ENO (WENO) which is a third-order accurate finite volume method. Later, Balsara and Shu (2000) provided a arbitrary-order accurate finite difference WENO scheme. Recently, some works (Hu *et al.*, 2016; Balsara *et al.*, 2016; Acker *et al.*, 2016; Borges *et al.*, 2008) have been developed with improvements to WENO implementation.

Instead of choosing just one candidate stencil to the reconstruction procedure like ENO, the WENO makes a convex combination of all candidate stencils. WENO uses a smoothness indicator based on the sum of the squares of L^2 norms. In the polynomial reconstruction the sub-stencils are multiplied for non-linear weights, which are inversely proportional to the smoothness indicator. In presence of a discontinuity the smoothness indicator will be higher and the weight tends to zero. In this way, WENO scheme achieve orders higher than ENO scheme for the same stencil.

2. GOVERNING EQUATIONS

The governing equations used to described the fluid dynamics of the investigated case are the well known Navier-Stokes equations for a viscous and compressible fluid. These are presented by Equations (1)-(3) and represents Mass

Conservation, the Momentum Transport and Energy Transport, respectively:

$$\frac{\partial \rho}{\partial t} + \frac{\partial \left(\rho u_i\right)}{\partial x_i} = 0, \tag{1}$$

$$\frac{\partial \rho u_j}{\partial t} + \frac{\partial \left(\rho u_i u_j\right)}{\partial x_i} = -\frac{\partial p}{\partial x_j} + \frac{\partial \tau_{i,j}}{\partial x_i}, \tag{2}$$

$$\frac{\partial \rho e}{\partial t} + \frac{\partial \left(\rho e u_i\right)}{\partial x_i} = -\frac{\partial p u_j}{\partial x_j} + \frac{\partial u_i \tau_{i,j}}{\partial x_j} + \frac{\partial}{\partial x_i}\left(\lambda \frac{\partial T}{\partial x_i}\right), \tag{3}$$

where, ρ is the density, u_i is the velocity component in i-direction, p is the pressure, T is the temperature and $\tau_{i,j}$ is the stress tensor, e is the total energy and λ is the thermal conductivity of the fluid.

Assuming Newtonian fluid, the stress tensor $\tau_{i,j}$ is defined as:

$$\tau_{i,j} = \mu\left(\left(\frac{\partial u_i}{\partial x_j} + \frac{\partial u_j}{\partial x_i}\right) - \frac{2}{3}\delta_{i,j}\frac{\partial u_k}{\partial x_k}\right). \tag{4}$$

The Energy Transport is based on the total energy, which is the sum of internal and kinetic energy. Assuming ideal gas, the total energy is defined as:

$$e = \frac{p}{\rho\left(\gamma - 1\right)} + \frac{1}{2}u_i u_i \tag{5}$$

where γ is the Poisson constant and is defined as the ratio of the heat capacity at constant pressure c_p to heat capacity at constant volume c_v:

$$\gamma = \frac{c_p}{c_v}. \tag{6}$$

The equation of state is used to compute the pressure:

$$p = \frac{\rho R T}{M}, \tag{7}$$

where $R = 8.314\ J \cdot mol^{-1} \cdot K^{-1}$ is the universal gas constant and M is the molar mass.

3. TURBULENT JET FLOW - TEST CASE

This preliminary study considered a subsonic heated planar jet of water vapour injected into a parallel cold coflow of water vapour. The velocity profile and temperature profile of the injected jet are given by Equations (8) and (9).

$$\frac{U_1 + U_2}{2} + \frac{U_1 - U_2}{2}\tanh\left(\frac{h/2 - |y|}{2\theta}\right), \tag{8}$$

$$\frac{T_1 + T_2}{2} + \frac{T_1 - T_2}{2}\tanh\left(\frac{h/2 - |y|}{2\theta}\right), \tag{9}$$

The temperature in the centerline of the heated jet is set to $T_1 = 860\ K$ and the temperature of the coflow is $T_2 = 380\ K$. The injected jet has velocity $U_1 = 8.34\ m/s$ in x-direction and no component velocity in y-direction and the width opening of the injected jet is $h = 0.05\ m$. The shear layer thickness is set to $\theta = 1.5 \times 10^{-3}$ This study was conducted in a two dimensional regular mesh of 400 points in x-direction and 350 point in y-direction on a domain of 0.6 meters in x-direction and 0.5 meters on y-direction. The inlet was set to be a Dirichlet boundary condition and the outflow was second-type boundary condition in which the derivatives of all properties were set to be zero.

4. NUMERICAL SCHEMES

In order to achieve high-order accuracy, the governing equations were numerically solved using the WENO scheme applied to the convective terms and 4^{th} order centered finite difference scheme applied to the diffusive terms.

4.1 WENO scheme

Considering the spatial derivative of a function f in a point j in x-direction by the difference between a high-order numerical flux F of the neighborhood of j divided by the cell size:

$$\frac{df_j}{dx} = -\frac{1}{\Delta x}\left(F_{j+1/2} - F_{j-1/2}\right). \tag{10}$$

Considering that this system has a complete set of eigenvalues and eigenvectors for the Jacobian of the flux in one direction, it is possible to project the fluxes of the conserved variables in a characteristic basis using the left eigenvectors. More details could be found in Shu and Osher (1989). The considered flux splitting is the Lax-Friedrich flux splitting giving by Equation (11):

$$\hat{f}^{\pm}_{j+1/2} = \frac{\lambda \cdot G_{j+1/2} \pm \alpha \cdot G_{j+1/2}}{2}, \tag{11}$$

where $G_{j+1/2}$ is the flux vector in the characteristic basis, λ is a vector of eigenvalues and α is the maximum absolute value of the eigenvalues.

Then, the WENO reconstruction is applied to each one of the characteristic fluxes found in Equation (11). The reconstructed polynomial of the numerical flux for fifth-order WENO scheme on cell $j + 1/2$ is giving by the convex combination of the sub-stencils below, that is:

$$\hat{f}_{j+1/2} = \omega_1 \hat{f}^{(1)}_{j+1/2} + \omega_2 \hat{f}^{(2)}_{j+1/2} + \omega_3 \hat{f}^{(3)}_{j+1/2}, \tag{12}$$

where the sub-stencils of third-order accuracy are giving by Equations (13)-(15)

$$\hat{f}^{(1)}_{j+1/2} = -\frac{1}{6}f_{j-1} + \frac{5}{6}f_j + \frac{1}{3}f_{j+1}, \tag{13}$$

$$\hat{f}^{(2)}_{j+1/2} = \frac{1}{3}f_j + \frac{5}{6}f_{j+1} - \frac{1}{6}f_{j+2}, \tag{14}$$

$$\hat{f}^{(3)}_{j+1/2} = \frac{11}{6}f_{j+1} - \frac{7}{6}f_{j+2} + \frac{1}{3}f_{j+3} \tag{15}$$

and the non-linear weights are giving by:

$$\omega_j = \frac{\alpha_j}{\sum_{k=0}^{3}\alpha_k}, \tag{16}$$

with,

$$\alpha_j = \frac{C_j}{(\varepsilon + \beta_j)}, \tag{17}$$

where ε is a constant to avoid division by zero, usually $\varepsilon = 10^{-6}$ and the linear coefficients are giving by:

$$C_1 = \frac{3}{10}, \quad C_2 = \frac{3}{5}, \quad C_3 = \frac{1}{10}. \tag{18}$$

The smoothness indicator for fifth-order WENO scheme on a regular mesh are giving by Equations (19)-(21):

$$\beta_1 = \frac{13}{12}\left(f_j - 2f_{j+1} + f_{j+2}\right)^2 + \frac{1}{4}\left(3f_j - 4f_{j+1} + f_{j+2}\right)^2, \tag{19}$$

$$\beta_2 = \frac{13}{12}\left(f_{j-1} - 2f_j + f_{j+1}\right)^2 + \frac{1}{4}\left(f_{j-1} - f_{j+1}\right)^2, \tag{20}$$

$$\beta_3 = \frac{13}{12}\left(f_{j-2} - 2f_{j-1} + f_j\right)^2 + \frac{1}{4}\left(f_{j-2} - 4f_{j-1} + 3f_j\right)^2. \tag{21}$$

After the WENO reconstruction the resulting right and left fluxes should be summed up to find the total characteristic flux crossing the cell boundary $j + 1/2$:

$$\hat{f}_{j+1/2} = \hat{f}^{+}_{j+1/2} + \hat{f}^{-}_{j+1/2}. \tag{22}$$

Using the right eigenvectors, orthonormal to the left eigenvectors, to bring back the fluxes in the characteristic basis to the physical one. Thus, the Equation (10) will be used to find the derivative of function. This procedure was applied on both directions to calculated de convective term used on time integration discussed below.

4.2 Time integration

The non-oscillatory schemes showed themselves a powerful tool to spatial discretization for discontinuous problems. Having said that, a TVD Runge-Kutta was developed and discussed in Shu (1988). This method was designed to maintain stability in the total variation norm. After the discretization of the convective and diffusive terms, one should integrate the Ordinary Differential Equation (23):

$$\frac{df_j}{dt} = L_j, \tag{23}$$

where *L* is function that synthesize the discretized convective and diffusive terms.

In order to maintain the high-order accuracy the third-order TVD Runge-Kutta, described by Equations (24)-(26), was used to time integration:

$$f^{(1)} = f^{(0)} + \Delta t \cdot L_1, \tag{24}$$

$$f^{(2)} = \frac{3}{4}f^{(0)} + \frac{1}{4}f^{(1)} + \frac{1}{4}\Delta t \cdot L_2, \tag{25}$$

$$f^{(3)} = \frac{1}{3}f^{(0)} + \frac{2}{3}f^{(2)} + \frac{2}{3}\Delta t \cdot L_3. \tag{26}$$

5. RESULTS

Preliminaries results shows that the simulations considering the currently WENO scheme implementation are in accordance with the current understanding of jet flows. Figures (1a) and (1b) shows the temperature and velocity component in x-direction, respectively, after 2.0 seconds after release. It is noted that the results presented in figures (1a) and (1b) show some expected characteristics of a real jet like fluctuations on properties fields. Curling shapes and the temperature gradient are well observed in the numerical findings. As the momentum is reduced the temperature difference increases which combined with the shear stress leads to zones of Kevin-Helmoltz instabilities. Mesh should be verified to ensure the grid spacing similar to the Kolmogorov scale and proper energy balance. In addition it is possible to notice the presence of oscillations near the centerline of the jet. Although the method used to discretize the convective terms was essentially non-oscillatory the derivatives present in the diffusive terms use a 4^{th} order centered scheme that introduces some spurious oscillations. An alternative to solve this problem would be to apply a filter to the entire solution or to use another discretization for the diffusive term.

Figures (1c) and (1d) shows a statistically stationary contours of temperature and x-component of the velocity, respectively. Figures (2a)-(2b) show profiles of temperature and x-component of the velocity of the stationary jet at a distance $x = h$ of the injection and figures (2c)-(2d) show profiles of temperature and x-component of the velocity of the stationary jet at a distance $x = 10h$ of the jet injection. The differences between the profiles at $x = h$ and $x = 10h$ shows that the jet tends tends to open and take the shape of a flat profile as the position is far enough of the injection. This behavior is an expected characteristics of jets.

6. ACKNOWLEDGEMENTS

The authors wish to thanks CAPES for the financial support.

7. REFERENCES

Acker, F., Borges, R.B.R. and Costa, B., 2016. "An improved weno-z scheme". *Journal of Computational Physics*, Vol. 313, pp. 726–753.

Balsara, D.S., Garain, S. and Shu, C.W., 2016. "An efficient class of weno schemes with adaptive order". *Journal of Computational Physics*, Vol. 326, pp. 780–804.

Balsara, D.S. and Shu, C.W., 2000. "Monotonicity preserving weighted essentially non-oscillatory schemes with increasingly high order of accuracy". *Journal of Computational Physics*, Vol. 160, pp. 405–452.

Borges, R., Carmona, M., Costa, B. and Don, W.S., 2008. "An improved weighted essentially non-oscillatory scheme for hyperbolic conservation laws". *Journal of Computational Physics*, Vol. 207, pp. 3191–3211.

Godunov, S.K., 1959. "Finite difference method for numerical computational of discontinuous solutions of the equations of fluid dynamics". *Matematicheskii Sbornik*, Vol. 47 (89), p. 271.

Harten, A., Engquist, B. and Osher, S., 1987. "Uniformly high order accurate essentially non-oscillatory schemes, iii". *Journal of Computational Physics*, Vol. 71, pp. 231–303.

Hewitt, E. and Hewitt, R.E., 1979. "The gibbs-wilbraham phenomenon: An episode in fourier analysis". *Archieve for History of Exact Sciences*, Vol. 21, pp. 129–160.

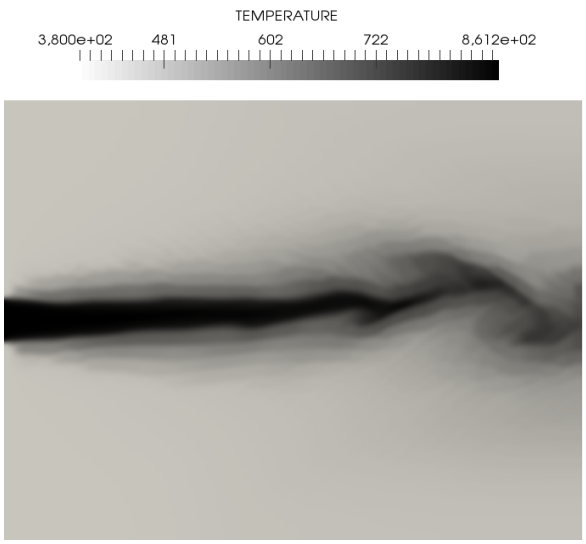

(a)

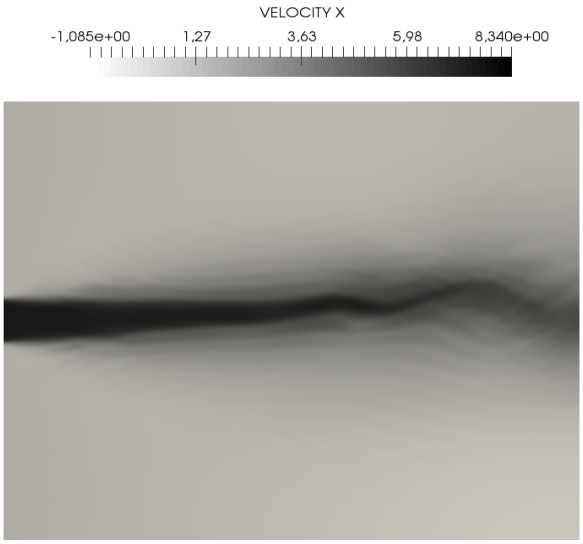

(b)

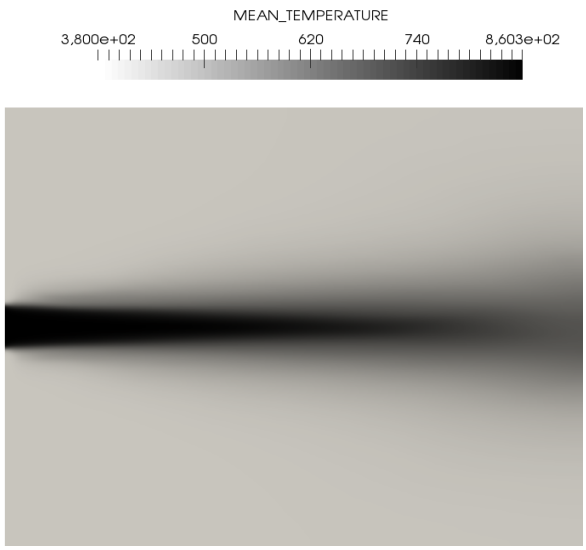

(c)

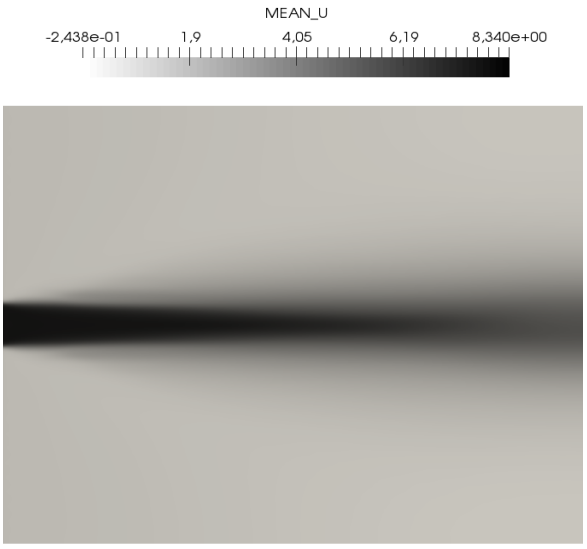

(d)

Figure 1: (a) Temperature contours for the turbulent jet flow 2.0 seconds after release. (b) Turbulent jet velocity contours 2.0 seconds after the release. (c) Mean temperature contour. (d) Mean x-velocity contour.

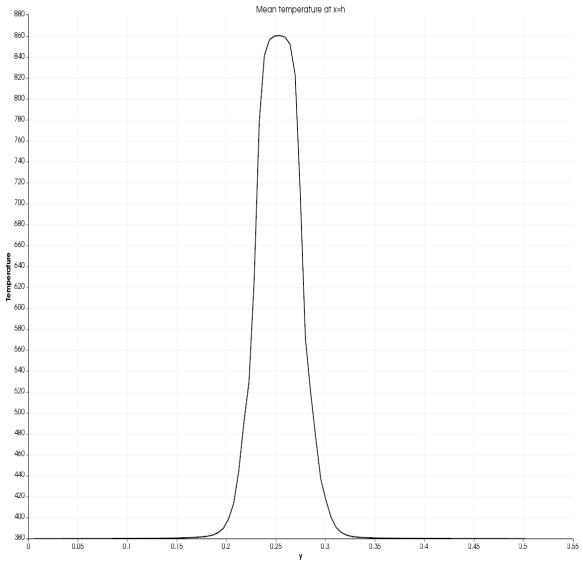

(a)

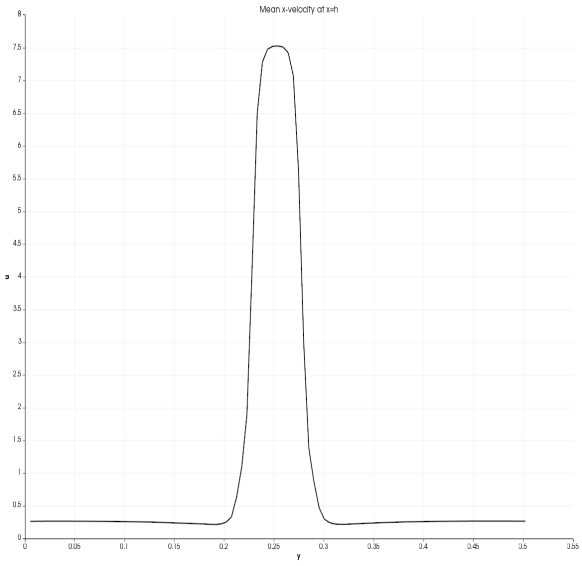

(b)

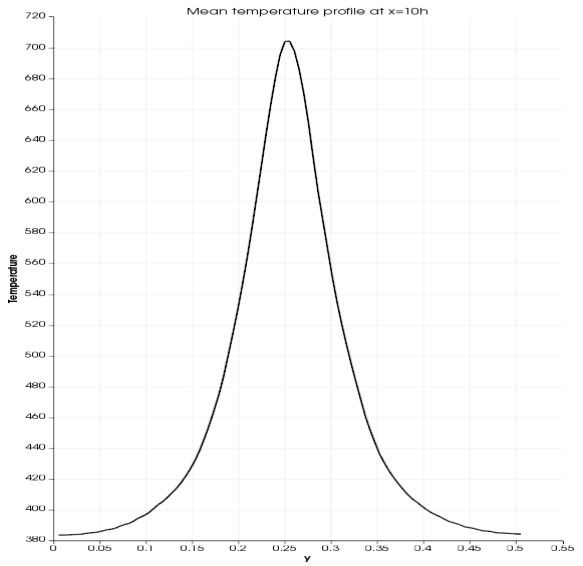

(c)

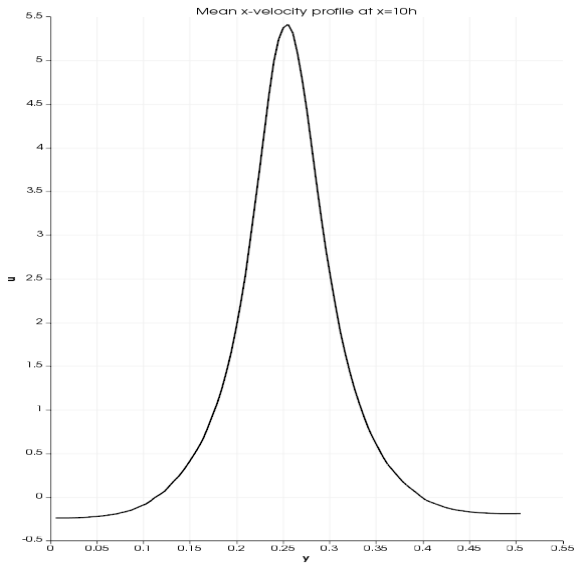

(d)

Figure 2: (a) Stationary jet temperature profile at $x = h$. (b) Stationary jet x-velocity profile at $x = h$. (c) Stationary jet temperature profile at $x = 10h$. (d) Stationary jet x-velocity profile at $x = 10h$.

Hu, F., Wang, R. and Chen, X., 2016. "A modified fifth-order wenoz method for hyperbolic conservation laws". *Journal of Computational and Applied Mathematics*, Vol. 303, pp. 56–68.

Liu, X.D., Osher, S. and Chan, T., 1994. "Weighted essentially non-oscillatory schemes". *Journal of Computational Physics*, Vol. 115, pp. 200–212.

Neumann, J.V. and Richtmyer, R.D., 1950. "A method for the numerical calculation of hydrodynamic shocks". *Journal of Applied Physics*, Vol. 21, p. 232.

Roe, P.L., 1981. "Approximate riemann solvers, parameter vectors, and difference schemes". *Journal of Computational Physics*, Vol. 43, pp. 357–372.

Shu, C.H., 2012. "On high-order accurate weighted essentially non-oscillatory and discontinuous galerkin schemes for compressible turbulence simulations". *Philosophical Transactions of the Royal Society A*.

Shu, C.W., 1988. "Efficient implementation of essentially non-oscillatory shock-capturing schemes". *Journal of Computational Physics*, Vol. 77, pp. 439–471.

Shu, C.W. and Osher, S., 1989. "Efficient implementation of essentially non-oscillatory shock-capturing schemes, ii". *Journal of Computational Physics*, Vol. 83, pp. 32–78.

8. RESPONSIBILITY NOTICE

The authors are the only responsible for the printed material included in this paper.